

# CMOS integrated antenna-coupled field-effect-transistors for the detection of 0.2 to 4.3 THz

S.Boppel<sup>a</sup>, A.Lisauskas<sup>a</sup>, D.Seliuta<sup>b</sup>, L.Minkevičius<sup>b</sup>, I.Kašalynas<sup>b</sup>, G.Valušis<sup>b</sup>, V.Krozer<sup>a</sup>, H.G.Roskos<sup>a</sup>

<sup>a</sup> Physikalisches Institut, Johann Wolfgang Goethe-Universität Frankfurt, Germany

<sup>b</sup> Semiconductor Physics Institute of Center for Physical Science and Technology, Lithuania

**Abstract** — Distributed phenomena permit the use of field-effect transistors for the detection of frequencies far beyond transistor cut-off. This contribution gives details on an improved design for patch antenna-coupled field-effect-transistors and shows sensitive detection from 0.2 to 4.3 THz for monolithically integrated devices relying on commercial 0.15- $\mu\text{m}$  CMOS process technology. Room-temperature responsivity values of 1344 V/W at 585 GHz, 90 V/W at 3.1 THz and 11 V/W at 4.3 THz are reported (values acquired at optimum operational point). A minimum optical noise-equivalent-power (NEP) of 163 pW/ $\sqrt{\text{Hz}}$  at 3.1 THz is reported (All values are normalized to the physical antenna area).

**Index Terms** — Submillimeter wave detectors, Terahertz detectors, patch antennas, CMOS, terahertz direct detection, distributed resistive self-mixing, plasmonic detection.

## I. INTRODUCTION

Common knowledge suggests that efficient application of transistors above their cut-off frequency is not feasible. While true for transit-time-limited applications such as amplification, this limitation becomes less strict when rectifying and mixing phenomena are considered. Based on plasma-wave phenomena occurring at frequencies larger than cut-off frequency, Dyakonov and Shur theoretically predicted in 1996 that field effect transistors can be applied to detection, mixing and even generation of THz radiation [1]. Subsequent experimental prove followed by subjecting discrete GaAs HEMTs to radiation with a frequency of 2.54 THz, which is 30-times above transistor cutoff [2]. For discrete silicon MOSFETs experimental quantification of rectification was carried out at 700 GHz in 2006 [3]. For practical purposes, we have shown that detection and mixing in MOSFETs in the overdamped case (valid for room temperature) can be understood as and modeled by distributed resistive self-mixing [4,5]. Based on this, first antenna-coupled detectors and few-pixel focal plane detector arrays for 645 GHz have been designed and implemented using a CMOS foundry process [4,5]. When compared to recently improved detectors, which have been fabricated in a 65 nm SOI process [6], we achieve similar performance values using an improved design while relying on cost-efficient 150 nm CMOS technology [7]. Improved detectors exhibit an minimum optical noise-equivalent-power (NEP) of 43 pW/ $\sqrt{\text{Hz}}$  and a maximum (capacitive-

loading-limited) optical responsivity of 970 V/W (both values averaged) at 590 GHz, excellent uniformity, low interchip variation of less than 8% between pixels, and achieve high yield [7]. Their low performance variations and their application to a 10-kilopixel camera testbed [8] suggest, that CMOS detectors are suitable candidates for commercial cameras applicable to imaging in fields such as non-destructive testing, quality control, medicine and security.

In this contribution, we give for the first time details to the modified circuit design which has also been used in [7]. This design results not only in improved performance, but also allows low frequency signals to be applied to the detector for calibration and to provide experimental access to important detector parameters. Secondly, we specifically used the modified design concept to realize antenna-coupled detectors for frequencies between 200 GHz and 4.3 THz in order to explore the high frequency behavior of the detection concept. We show characterization results demonstrating sensitive detection for frequencies up to 4.3 THz.

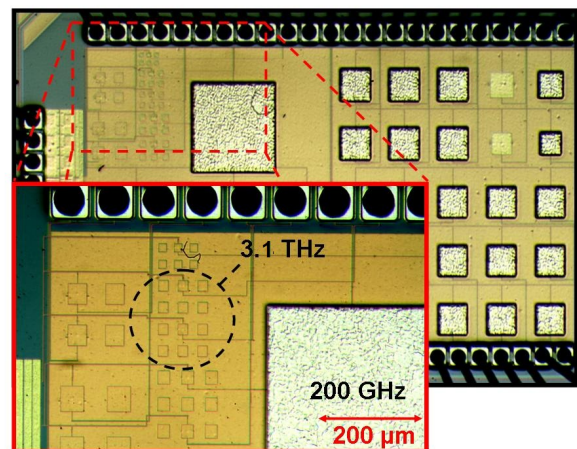


Fig. 1. A micrograph of a 1.5 x 2.5 mm<sup>2</sup> large silicon die showing different patch antennas targeted for various THz frequencies. A close-up photograph showing the high frequency section (for frequencies larger than 1.4 THz) of the chip as well as a part of a 200 GHz antenna.

## II. DESIGN AND LAYOUT

Detectors targeted for various THz frequencies were fabricated on a  $1.5 \times 2.5 \text{ mm}^2$  large silicon die (see Fig. 1) using the 150-nm CMOS process provided by LFoundry GmbH.

### a) The Detector Circuit

A detector consists of a monolithically integrated patch antenna connected to a pair of transistors as rectifying elements in a differential configuration. Figure 2 illustrates the design of a 590 GHz detector, which in contrast to earlier implementations described in [4,5], couples the radiation directly to the drain terminal and reads out the rectified signal at the center of the patch antenna, which acts as virtual ac ground. The gates of both transistors are connected ensuring that they are coupled to an ac ground, and an external dc voltage  $V_{gs}$  can be applied for the control of the charge carrier density in the transistors' channels. This design exhibits a couple of advantages. By reading out the detector at the antenna center (ac ground), the antenna itself acts as a low-pass filter and, therefore, additional lossy filter structures can be avoided. The transistors are placed in proximity to the antenna feed, therefore, transmission line losses can be reduced. This simplification and the avoidance of long transmission line structures could also be beneficial for obtaining such low performance variations [7] among different detectors. Additional to above mentioned advantages on the detector characteristic, the described design allows also to electronic apply and detect low frequency signals using the readout port. Although the detector is then operated in a different (low frequency) regime, detection persists as classical resistive self-mixing. By understanding the relation of both regimes, low frequency measurements currently prove quite valuable for experimentally obtaining knowledge about important devices parameters, for gaining insight into physical phenomena at THz frequencies and for detector calibration (We are currently working on these topics).

### b) Antenna considerations

Essential for highly sensitive detection performance is a proper antenna implementation. A lossy silicon substrate and the limited thickness of the back-end complicate the design of antennas when a standard CMOS process is used. However - to the surprise of many - when going beyond 1 THz, antenna implementation becomes less challenging: For example, the LFoundry process, which we use, offers approximately a  $7 \mu\text{m}$  thick dielectric between the metal layers 'M1' and 'Top Metal'. The ratio between this thickness and the wavelength in material

stays below 1% for frequencies lower than 200 GHz, which constitutes a hard challenge to antenna designers. However, going to larger frequencies this design constraint gradually relaxes and at 4.3 THz a thickness to wavelength ratio of 20% is reached. Thus, at larger frequencies antennas not only take up less silicon but also the gained design freedom allows to implement more favorable and efficient antenna structures.

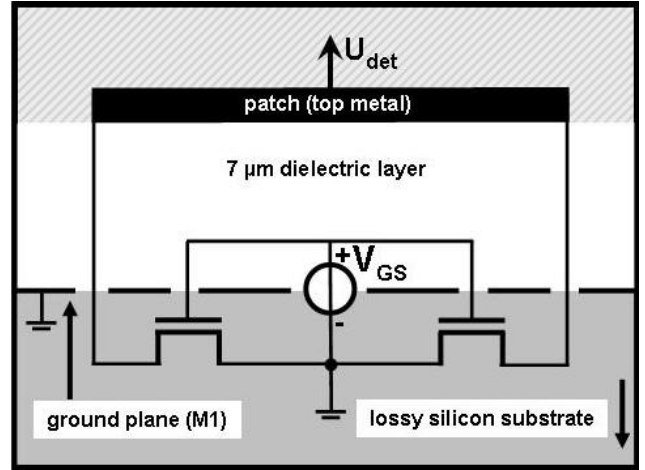


Fig. 2. Schematic cross-section of patch-antenna-coupled differential pair of field effect transistors for the detection of 590 GHz (not to scale). The antenna is also used for signal read out.  $V_{gs}$  – external gate bias voltage.

### c) Layout of the 0.2 to 4.3 THz Chip

Figure 1 shows a micrograph of the  $1.5 \times 2.5 \text{ mm}^2$  large silicon die. Detectors have been implemented for various target resonance frequencies in the THz range (200 GHz, 300 GHz, 555 GHz, 590 GHz, 693 GHz, 824 GHz, 1.4 THz, 1.6 THz, 2.5 THz, 3.1 THz and 4.3 THz). Frequencies below 600 GHz are tailored to our electronic sources while frequencies above 600 GHz are tailored to the discrete emission frequencies of a  $\text{CO}_2$ -pumped gas laser. A patch antenna for 590 GHz has been simulated using CST microwave Studio with an antenna impedance at resonance of about  $300 \Omega$ . The -3dB bandwidth of the antenna is 8% [6]. For the sake of comparability of the efficiency of the detection principle across the THz range, the 590 GHz patch antenna were rather rescaled than us making use of above mentioned additional design freedom offered by the CMOS back-end at larger frequencies. From table 1 the patch size and metal layer of the patch can be extracted for selected antennas. The ground plane is kept on metal M1 for all detector designs. In Figure 1, the scaling of antenna dimensions becomes evident when the 200 GHz and the 3.1 THz antennas are compared. As the antenna size scales with the square of the wave length,

multi-pixel cameras would require significantly less chip space at larger frequencies.

### III. RESULTS

Detectors optimized for 590 GHz have been thoroughly characterized in [5] showing a maximum (capacitive-loading-limited) optical responsivity of 970 V/W and a minimum optical noise-equivalent-power (NEP) of 43 pW/ $\sqrt{\text{Hz}}$  at room temperature (both values averaged over 15 samples on different chips). The performance of the detectors has a low standard deviation of less than 8%. The detector performance can be further improved when cryogenically cooled until the carrier freeze-out is reached. This improvement occurs because of two reasons: (i) with the decrease of temperature also the amplitude of thermal noise decreases, and (ii) the nonlinear dependence between carrier density and local electric field increases. At 20 K, detectors with an antenna resonant at 590 GHz can reach a maximum responsivity of 3.47 kV/W and a NEP as low as 3 pW/ $\sqrt{\text{Hz}}$  at this frequency. It should be noted that values reported so far are based on the self-referenced procedure described in Ref. [9] and have been normalized to the detector area. As these 590 GHz detectors have been arranged in as a detector focal plane array, the antenna pitch was used to determine the detector area. All following values, including values in the figures, will be normalized to the physical area of the antenna (antenna patch size). As not all designed detectors shown in Fig. 1 have been arranged in an array, the antenna pitch as the area of a detector pixel is not applicable anymore. Responsivity and NEP values need to be rescaled by a factor of 3.6 to estimate the values for pixels in a focal plane array normalized to the pitch.

Before discussing the detectors designed for frequencies up to 4.3 THz, further results on the 590 GHz detector pixel are presented when characterized across a wide range of discrete frequencies provided by a CO<sub>2</sub>-pumped gas THz laser. When the gas THz laser is used, characterization is based on power density estimates of the focal spots. This characterisation method has been confirmed by the self-referenced procedure described in Ref. [9]. Good sensitivity can be observed at the main antenna resonance and also at the third harmonic of the main resonance (black circles in Figure 3). Responsivity values of 1344 V/W at 584 GHz and 77 V/W at 1.8 THz are obtained in contrast to 1.2 V/W at 1.4 THz when the detector is used off antenna resonance. Transistor detectors are biased to the point of the lowest NEP ( $V_{\text{gs}} = 0.7$  V). It shall be stressed that the two resonances purely originate from antenna properties.

Now, we explore the performance of detectors with target frequencies larger than 600 GHz, which have also been characterized using at CO<sub>2</sub>-pumped gas THz laser. The measured optical responsivity values are shown in Figure 3.

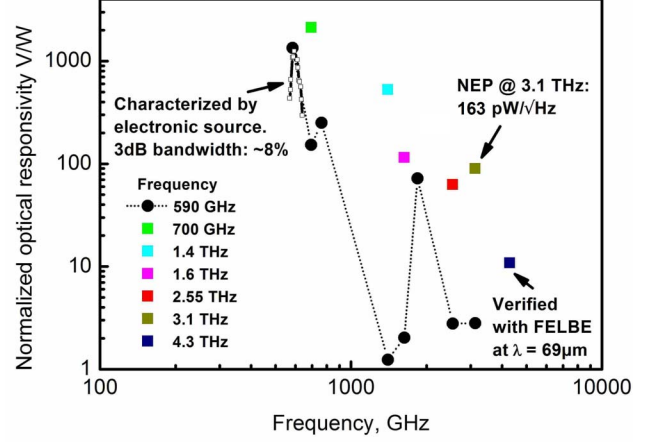


Fig. 3. Optical responsivity of detectors designed for discrete frequencies of a CO<sub>2</sub>- laser. A pixel with a main resonance at 590 GHz (black) exhibits good sensitivity at the third harmonic. Note: The optical responsivity is normalized to the detector patch rather than the detector pitch.

| Patch size          | Metal layer | Frequency | Resp | NEP                    |
|---------------------|-------------|-----------|------|------------------------|
| ( $\mu\text{m}^2$ ) | -           | (THz)     | V/W  | pW/ $\sqrt{\text{Hz}}$ |
| 109x118             | MT          | 0.590     | 1344 | 11                     |
| 92x100              | MT          | 0.694     | 2126 | 6.9                    |
| 45x49               | M4          | 1.4       | 528  | 28                     |
| 19x21               | M3          | 3.1       | 90   | 163                    |
| 15 x 16             | M2          | 4.3       | 11   | 1330                   |

Table 1. Detectors differ in ‘patch sizes’, ‘metal layer’ of integrated patch and have been characterized discrete ‘frequencies’. Optical responsivity and NEP have been obtained at gate bias of 0.7V and been normalized to detector patch size.

Detectors explicitly designed for 0.585, 0.694, 1.4, 1.6, 2.5, 3.1 and 4.3 THz have optical responsivities of 1344, 2126, 528, 115, 69, 90 and 11 V/W, respectively. The off-resonance values of the 590 GHz detector can again be used for comparison. THz detection with silicon-based FETs is maintained up to 4.3 THz. The 4.3 THz measurement has been confirmed with the free electron laser FELBE at the HDRZ, Dresden-Rosendorf ( $\lambda=69\mu\text{m}$ ). Despite these remarkable results, we still believe that these values underestimate detector performance at the actual antenna resonance, which might have slightly been missed by the discrete frequency of the

incident radiation as the antenna bandwidth is typically 8% from center frequency. In Figure 3 the spectral response for a 590 GHz pixel is shown. To obtain the full spectral responsivity of the detectors and the peak performance values of the detectors, measurements with frequency tunable THz sources are currently being planned and will make a quantitative analysis of the roll-off possible. Parasitic impedance estimations performed at 590 GHz estimate an even smaller performance frequency roll-off of silicon-based detectors of the current design. Responsivity in the vicinity of 4.3 THz could reach up to 100 V/W. This argument is also supported by the outstanding result at 3.1 THz, where a responsivity of 90 V/W and a NEP value of 163 pW/ $\sqrt{\text{Hz}}$  are reached as is listed in table 1. The results are a strong indication that detection concept up to 4.3 THz is mainly limited by devices parasitic rather than physics. Parasitics can still be reduced by using a more advanced process technology.

At first glance such a high responsivity at frequency values, which exceed transistors cut-off frequency in the order of 100 times is unexpected, however, is possible because of the plasma wave-nature of the rectification process in contrast to the conventional transport-based nonlinear rectifiers.

#### IV. CONCLUSION

In conclusion, we have integrated detectors for frequencies from 0.2 to 4.3 THz using a commercial 0.15- $\mu\text{m}$  CMOS process technology and utilizing an improved device designs of patch antenna-coupled field-effect-transistors. Experimental room-temperature responsivity values of 1344 V/W at 585 GHz, 90 V/W at 3.1 THz and 11 V/W at 4.3 THz we show that the detection concept persists deep into the THz gap and does not seem to be limited by physics as transport-based rectifiers are. Also CMOS back-end literally leaves room for improvement by relaxing design constraints at higher frequencies. With this in mind intrinsically fast electronic components seem feasible deep in the THz gap, which not only would render possible single color cameras, but also spectroscopic sensors based on frequency selective antennas tailored for various frequencies.

#### ACKNOWLEDGEMENT

Funding was provided by BMBF project LiveDetect3D, Oerlikon AG, Alexander von Humboldt-Foundation and by WI Bank Hessen. We are grateful for the organizational support by Innovectis GmbH and thank Martin Mittendorff and Stephan Winnerl from FELBE for their support.

#### REFERENCES

- [1] M. Dyakonov and M. Shur, "Detection, mixing, and frequency multiplication of terahertz radiation by two-dimensional electronic fluid," *IEEE Trans. Electron. Devices*, vol. 43, pp. 380-387, 1996.
- [2] Jian-Qiang Lü; Shur, M.S.; Hesler, J.L.; Liangquan Sun; Weikle, R.; , "Terahertz detector utilizing two-dimensional electronic fluid," *Electron Device Letters, IEEE* , vol.19, no.10, pp.373-375, Oct 1998
- [3] R. Tauk, F. Teppe, S. Boubanga, D. Coquillat, W. Knap, Y. M. Meziani, C. Gallon, F. Boeuf, T. Skotnicki, T. Skotnicki, C. Fenouillet-Beranger, D. K. Maude, S. Rumyantsev, and M. S. Shur, "Plasma wave detection of terahertz radiation by silicon field effects transistors: Responsivity and noise equivalent power," *Appl. Phys. Lett.*, vol. 89, p. 253511, 2006.
- [4] A. Lisauskas, U. Pfeiffer, E. Öjefors, P. Haring Bolívar, D. Glaab, and H. G. Roskos, "Rational design of high-responsivity detectors of terahertz radiation based on distributed self-mixing in silicon field-effect transistors," *J. Appl. Phys.*, vol. 105, p. 114511, 2009.
- [5] Öjefors, E., Pfeiffer, U., Lisauskas, A., and Roskos, H.G., 'A 0.65 THz focal-plane array in a quarter-micron CMOS process technology', *IEEE J. Solid-State Circuits*, 2009, 44, (7), pp. 1968-1976.
- [6] Öjefors, E., Baktash, N., Zhao, Y., Al Hadi, R., Sherry, H., and Pfeiffer, U.: 'Terahertz imaging detectors in a 65-nm CMOS SOI technology', *IEEE European Solid-State Circuits Conference*, Seville, Spain, September 2010, pp. 486 – 489. H. Sherry, R. Al
- [7] S. Boppel, A. Lisauskas, V. Krozer and H. G. Roskos, "Performance and performance variations of sub-1-THz detectors fabricated with a 0.15- $\mu\text{m}$  CMOS foundry process," *Electron. Lett.* 2008, 47, (11), 661-662.
- [8] S. Boppel, A. Lisauskas, A. Max, V. Krozer and H. G. Roskos, "CMOS detector arrays in a 10-kilopixel camera testbed for coherent terahertz real-time imaging," submitted to *Optics Letters*.
- [9] A. Lisauskas, D. Glaab, H. G. Roskos, E. Öjefors, and U. R. Pfeiffer, "Terahertz imaging with Si MOSFET focal-plane arrays", *Proc. SPIE.*, 2009, 7215, 72150J.